EFFECT OF A CNT INTERFACE IN IMPROVING THERMAL CONDUCTANCE OF CONTACTING SURFACES

Shadab Shaikh, University of Dayton, Dayton, OH, 45459, USA
Khalid Lafdi, University of Dayton, Dayton, OH, 45459, USA
Edward Silverman, Northrop Grumman Space Technology, One space Park, Redondo Beach, CA, 90278,USA

Experimental and theoretical analyses were used to study the effect of thermal contact resistance in two materials, aluminum and graphite. Experimental investigation included the use of a modern laser flash device to measure the effective thermal conductivity of each material for three different cases: in direct contact, with a graphite coating and with a thin sheet of carbon nanotube (CNT) thermal interface material (TIM). For both materials total thermal resistance values were determined corresponding to different cases for same contact pressure. Results showed that the CNT TIM produced the minimum thermal contact resistance. A theoretical study was carried out to compare the experimental results with thermal resistance models from the literature. Based on the surface roughness of the materials tested, two models were used. Both models showed reasonable agreement with the experimental results with an error of less than 6.5 %. The results demonstrate the effectiveness of CNT materials in improving the thermal conductance of contacting surfaces.

Introduction

Heat dissipation is the most critical problem that limits the performance, power, reliability and further miniaturization of microelectronics. The thermal performance of these devices is greatly affected by the thermal resistance associated with interface between the heat sink and heat source. The improvement of a thermal contact is associated with a decrease of the thermal resistance imposed by this interface as the heat flows across it (Oulette and Sargo 1985, Vogel 1995, Sartre 2001). As surfaces are never perfectly flat, the interface comprises point contacts at asperities and air pockets. Some heat is conducted through the physical contact points, but much more is transmitted through the air gaps. Since air is a poor conductor of heat, it should be replaced by a more conductive material to increase the joint conductivity and thus improve heat flow across the thermal interface. Use of suitable interface materials can thus have a significant role in lowering thermal contact resistance.

The main objective of thermal management in many applications is the efficient removal of heat from the semiconducting device to the ambient environment. The interface between any two contacting surfaces is generally neither fully conforming nor smooth. Rather, the surfaces are somewhat non-conforming and rough making the real contact area between the package and the heat sink is substantially smaller than the corresponding nominal contact surface area. Consequently, the heat transfer across the device/heat sink interface takes place through surface-asperity microcontacts and through air-filled micro-gaps (Figure 1), and is, hence, associated with a significant thermal resistance or thermal contact resistance Grujicic et al., 2005.

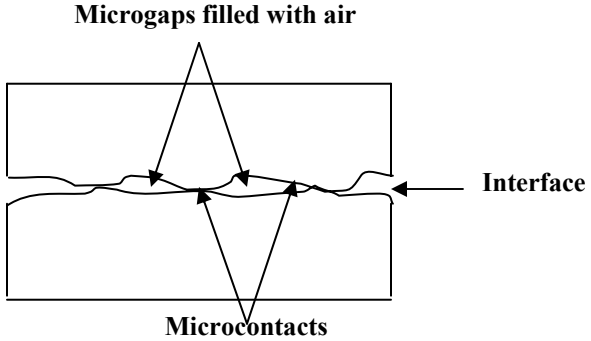

Figure 1. Enlarged view of an interface for any two contacting surfaces

To reduce the thermal resistance between contacting surfaces different variety of materials commonly referred as thermal interface materials have been developed (Wilson et al. 1996, Peterson 1990, Sasaki et al. 1995 Xu et al. 2002, Xu et al. 2000) . These materials are used to reduce or completely eliminate the air gaps from the contact interfaces by conforming to the rough and uneven mating surfaces. Because the thermal interface materials generally possess a higher thermal conductivity than the interfacial gas (air) they replace, the interfacial thermal resistance is reduced giving rise to a lower temperature of the electronic component junction. The efficiency of the thermal interfacial materials in reducing the interfacial thermal resistance depends on a number of factors among which thermal conductivity of the material and its ability to wet the mating surfaces appear to be the most significant.

Carbon nanotubes (CNT) with their light weight and high thermal conductivity value have the potential to be used as thermal interface material. The high intrinsic thermal conductivity of CNT (Berber et al. 2000, Che at al. 2000, Kim et al. 2001, Maruyama et al. 2003) suggests many heat transfer enhancement applications. Choi et al. 2001 measured the effective thermal conductivity of nanotube-in-oil suspensions and found that, with 1 vol% of nanotubes, the effective thermal conductivity increased significantly (more than twice the value of the base oil) though not nearly as much as a simple, above-threshold percolation model would predict, Huxtable et al. 2003. Recently, Xu and Fisher 2004 have shown that the thermal contact resistance between silicon wafers and copper with a CNT array interface can be as low as 23 mm2 K/ W. They also have shown that CNT arrays with different properties produce measurable variations in thermal enhancement. Thus the CNT can play a significant role in reducing the thermal resistance by lowering or eliminating the micro-gaps at the same time providing a high thermal conductivity path through them.

The twofold focus of this study is first, to study the effect of thermal contact resistance on heat transfer capability of high thermal conductivity materials and second is to demonstrate the effectiveness of CNT as thermal interface materials.

Materials Fabrication

Using quartz as the substrate, we managed to grow aligned CNTs with thickness ranging from several micrometers to about 200 um with a narrow diameter distribution around 15 nm. The thickness was monitored precisely by the growth time. The growth time was varied between 10 to 30 min.

Scanning electron microscopy characterization showed that CNT film is made of nanotube with homogenous length and diameter about 10nm. However use of Raman spectroscopy showed that aligned CNT film was made of mixture of single and multiwalled carbon nanotubes (Figure 2).

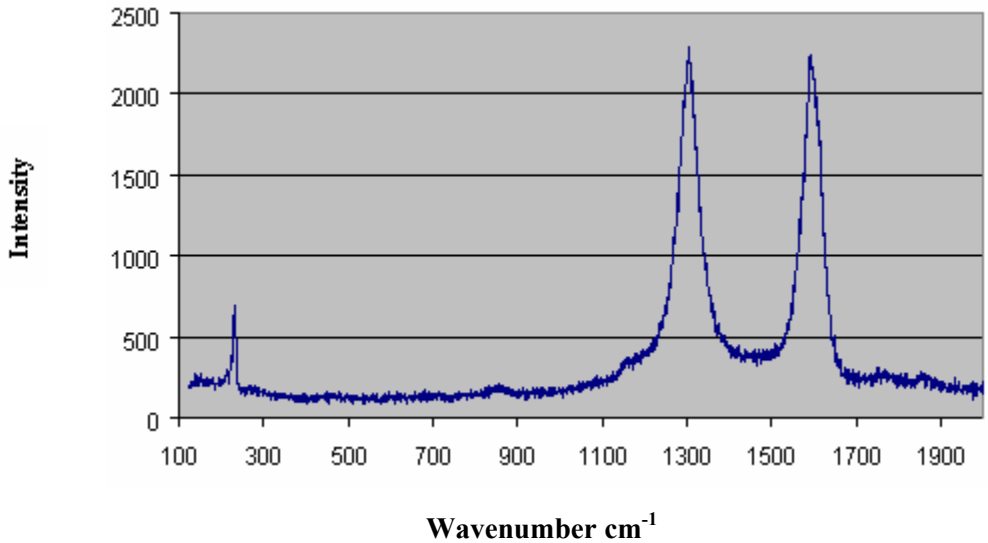

Figure 2. Raman spectrum of vertically aligned single-walled and multi-walled CNTs

Even though our process was focused on making 100% multi-walled carbon nanotubes (MWNTs) it produced a mixture of single-walled carbon nanotubes (SWNTs) as well. The most important feature in the Raman spectrum of CNTs is the Radial Breathing Mode (RBM), which is usually located between 75 and 300 cm^{-1} from the exciting line; an illustration of the spectrum resulting from this mode is displayed in the Figure 2. Since SWNTs are subject to inter-tube interactions which increase the frequency of the RBM, the D mode (disorder band located between 1330-1360 cm^{-1} when excited with a visible laser) is expected to be observed in (MWNTs). However when it was observed in SWNTs, it was assumed that this is due do defects in the tubes. The G mode or tangential mode corresponds to the stretching mode in the graphite plane. This mode is located around 1580 cm^{-1}.

Experimental analysis

Measurements, results and discussion

The experimental work involved the use of a modern light flash apparatus (LFA 447) in measuring the thermal diffusivity of different samples analyzed with and without thermal interface material. The LFA 447 is a modern contact-free laser flash method used for the measurement of thermal diffusivity of both solids and liquids. The thermal diffusivity measuring range is 0.01 to 1000 mm^2/s with reproducibility of approximately $\pm$ 3%. In addition to the thermal diffusivity, by employing a comparative method, the specific heat can also be determined with this apparatus by using a known sample as the reference. For the specific heat, a reproducibility of $\pm$ 5% is achieved. If the bulk density is known, a direct determination of the thermal conductivity is possible. The thermal conductivity range is 0.1 to 2000 W/mK.

Two types of materials were analyzed for thermal contact analysis,

- Aluminum (High thermal conductivity material)
- Graphite (Very high thermal conductivity material)

The value of density was first determined for all the materials by measuring the weight of sample and its size. Now for each type of material four different tests were carried out. In the first case a single sample piece for each material with size 10mm x 10 mm and 1.6 mm thickness was measured for its thermal diffusivity on the LFA. For the second case two similar sized pieces for the same material were kept in surface to surface contact, (Figure 3a) and the thermal diffusivity of the combined sample was measured. For the third case a graphite coating was provided between the two sample pieces and the thermal diffusivity of the combined sample was measured, (Figure 3b). Finally for the fourth case a thin sheet of CNT TIM was sandwiched between the two sample pieces and once again the thermal diffusivity of the combined sample was measured, (Figure 3c). A few drops of acetylene were added on the CNT sheet to have better wetting at the interface and then dried off. In a similar manner specific heat was measured for all the four type of cases for each material. All the measurements were carried out at a temperature of 25 $^{\circ}C$.

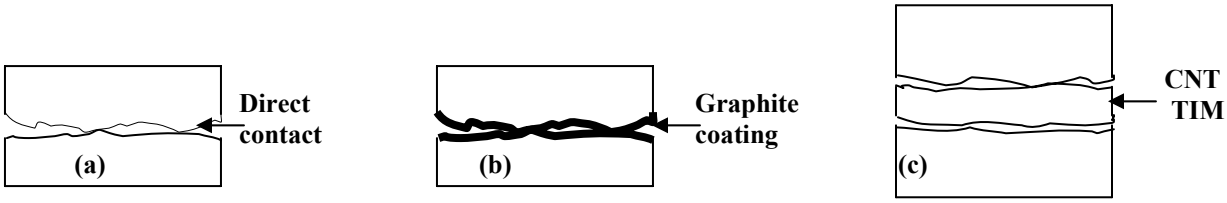

Figure 3 Schematic of contacting surfaces: (a) in direct contact (b) separated by graphite coating (c) separated thin sheet of CNT interface material.

The following table 1 gives the thermal conductivity for aluminum and graphite respectively with the percent enhancements.

Table 1 Measured thermal conductivity values for aluminum and graphite samples with their percentage enhancements.

Sample type	Thermal conductivity (W/m.K)	Enhancement (%)
Aluminum solid	95.73	--
Aluminum pieces in direct contact	8.957	--
Aluminum pieces with graphite interface	37.983	324.06
Aluminum pieces with CNT interface	43.457	385.16
Graphite solid	102.066	--
Graphite pieces in direct contact	13.475	--
Graphite pieces with graphite interface	50.033	271.80
Graphite pieces with CNT interface	62.278	362.79

The samples used for graphite materials were finely polished pieces on the other hand the aluminum samples were polished with sand paper. All the combined samples were subjected to a same load creating a contact pressure of 0.025 Mpa.

For the aluminum samples a huge drop in thermal conductivity was observed for aluminum pieces in direct contact. With the coating of graphite a rise of over 300 % was observed. Finally with the introduction of CNT interface material an enhancement of more than 350 % was obtained.

For the graphite samples also considerable drop in thermal conductivity was observed for surfaces in direct contact. With the introduction of graphite coating an increase of over 250 % was obtained and by the insertion of CNT interface material an even higher enhancement of more than 350 % was observed.

It was obvious from results that without any interface material air trapped in the microgaps created a thermal resistance bringing down the thermal conductivity. The effect of micro airgaps was more pronounced for the case of aluminum with relatively rough surface as compared to graphite. The finely polished surface of graphite materials created a better contact at the interface. From the thermal conductivity values obtained from the experiments for all three materials the CNT TIM produced the greatest enhancement. The thin CNT sheet TIM helped in providing a high conductivity heat transfer path thus minimizing the effect of micro airgaps resistance. However, it was clear that by combining the CNT sheet with a material with high wetting characteristic (phase change thermal interface material) a better contact can be achieved especially for the aluminum samples with rough surface.

The next task was to estimate the total thermal resistances corresponding to the conductivity values obtained for the aluminum and graphite samples, which were determined as shown in table 2 below. From this table it can be seen that for all the materials tested the inclusion of first the graphite coating and then the CNT sheet interface material helped in reducing the thermal contact resistance. Both the high thermal conductivity materials (aluminum and graphite) experienced a greater thermal interface resistance without the inclusion of interface material. This may be due to the huge drop in heat flux at the interface consisting of air gaps. Also, the relatively rough surface of the aluminum sample caused a slightly greater resistance which means that for the same contact pressure the use of smooth mating surfaces in place of rough ones increases the thermal contact conductance. This is consistent with previous work of Luo et al. 2002, and is due to the relatively small size of air pockets for the case of smooth surfaces. However, the case of rough surfaces is closer to the situation in microelectronics.

Table 2 Experimentally determined values of total thermal resistances for aluminum and graphite samples

Sample type	Thermal resistance (K/W)
Aluminum pieces in direct contact	3.573
Aluminum pieces with graphite interface	0.842
Aluminum pieces with CNT interface	0.736
Graphite pieces in direct contact	2.523
Graphite pieces with graphite interface	0.679
Graphite pieces with CNT interface	0.562

Theoretical model

In order to compare the experimental results with some of the thermal resistance models from the literature a theoretical study was carried for the two materials tested. The theoretical models were selected based on the roughness characteristics of the sample surfaces. Accordingly the total thermal resistance of relatively rough aluminum samples ($0.8\mu m$) was determined using the model based on micro-contacts, Savija et al. 2002 and Teertstra et al. 1999. For the case of polished graphite samples with surface roughness values of $0.121\mu m$ the general theoretical model based on the work of Veziroglu, 1967 was implemented.

Thermal resistance calculations for aluminum

Thermal joint resistance at the interface is a function of several geometric, physical and thermal parameters such as surface roughness and waviness, surface micro-hardness, thermal conductivity of the contacting solids, properties of the interstitial materials, and the contact pressure. The thermal resistance of a joint formed by two nominally flat rough surfaces (Figure 4.) can be obtained from a model that is based on following simplifying assumptions:

- Surfaces are nominally flat and rough with Gaussian height distributions.
- The load is supported by the contacting asperities only.
- The load is light; nominal contact pressure is small; $P/H_c \approx 10^{-3} to 10^{-5}$

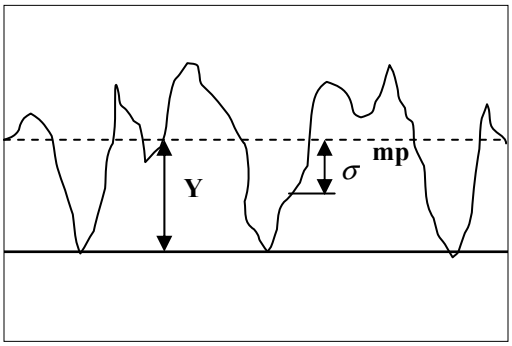

Figure 4. Equivalent rough surface and smooth plane contact

In general, the joint thermal conductance h_j and joint thermal resistance R_j depends on the contact and gap components.
The joint conductance is modeled as,

$$h_j = h_c + h_g \tag{1}$$

The joint resistance is modeled as:

$$\frac{1}{R_j} = \frac{1}{R_c} + \frac{1}{R_g} \tag{2}$$

where, R_c is the micro-contact resistance and R_g is the gap resistance.
The equation for was as used by Shaikh and Lafdi (2007) is given by,

$$R_j = \left[\left\{ 1.25 K_s \left(\frac{m}{\sigma} \right) \left(\frac{P}{H_c} \right)^{0.95} + \frac{k_g}{Y + M} \right\} A_a \right]^{-1} \tag{3}$$

The above relation was used to calculate the thermal contact resistance R_j for the combined aluminum samples.

Now the total thermal resistance R_T was calculated based on the Figure 5 for the aluminum samples using the relations below.

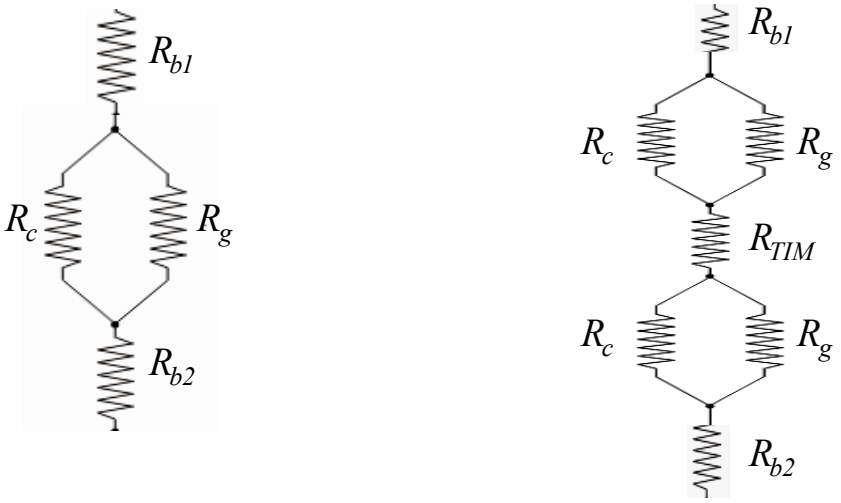

Figure 5. Equivalent thermal resistance circuit for: (a) Contacting surfaces in direct contact and separated by graphite coating (b) Contacting surfaces separated by thin sheet of TIM (CNT)

With a direct contact and with graphite coating,

$$R_T = R_{b1} + R_j + R_{b2} \tag{4}$$

With CNT interface material,

$$R_T = R_{b1} + R_j + 2R_{TIM} + R_{b2} \tag{5}$$

where, R_{b1} and R_{b2} are the thermal resistances through the bulk solid pieces in contact

Thermal resistance calculations for graphite

Various theories have been formulated to predict thermal conductance for a variety of conditions. Agreement with experiments has been variable (Rohsenow and Hartnett 1973, Ochterbeck 1991) especially when very smooth surfaces are involved. In order to correlate the analytical and measured contact conductance it is first necessary to measure and quantify the finish of the opposing surfaces. For rougher surfaces and if one or both of the surfaces is composed of a material that can deform easily at either the microscopic or macroscopic level then the pressure can affect the contact conductance. While discrepancies are often due to lack of precise input parameters Wolff and Schneider 1998 showed that a general theory could be modified to give a good estimation of the thermal resistance with a variety of interface materials.

Now the general model for interface thermal conductance is based on work of Veziroglu, 1967. An effective gap thickness is described by,

$$\delta = N(\delta_1 + \delta_2) \tag{6}$$

where N equals the slope of a best fit line through the empirical data points of the sum of surface roughness versus the effective gap thickness Veziroglu determined $N=3.56$ for $(\delta_1 + \delta_2) < 7\mu m$ and 0.46 if $> 7\mu m$.

The effective fluid thermal conductivity is determined by, $k_f = k_o$ if the interstitial fluid is liquid and,

$$k_f = \frac{k_o}{1 + \frac{8\gamma(\nu/\upsilon')(a_1 + a_2 - a_1 a_2)}{100\delta \Pr a_1 a_2(\gamma+1)}} + \frac{4\sigma\delta E_1 E_2 T_m^3}{E_1 + E_2 - E_1 E_2} \quad (7)$$

if it is a gas.
Now the conduction number *K* is found from relation

$$K = k_f \left[\frac{k_1 + k_2}{2k_1 k_2} \right] \quad (8)$$

The constriction number C is defined as,

$$C = \sqrt{\frac{P}{M}} \quad (9)$$

while the interface number S is,

$$S = \frac{\sqrt{A}}{\delta} \quad (10)$$

The gap number *B* is the relationship between the constriction number and the interface size number given by,

$$B = 0.335 C^{0.315 S^{0.137}} \quad (11)$$

The conductance number *U* can be found by the iteration of the following transcendental equation,

$$U = 1 + \frac{BC}{K \tan^{-1}\left\{(1/C)(1-(1-U))^{0.5} - 1\right\}} \quad (12)$$

or graphically from the chart for thermal contact conductance using *C* and *B/K*.
the thermal contact conductance *u* is thus given by relation,

$$u = \frac{h}{A} = \frac{Uk_f}{\delta} \quad (13)$$

Thus, the joint thermal contact resistance for the polished surface can be obtained from the relation,

$$R_j = \frac{1}{u} = \frac{\delta}{Uk_f} \quad (14)$$

Wolff and Schneider 1998 used the above model for thermal contact conductance and noticed the discrepancy between their measured and predicted values based on the expression for the effective gap thickness given by equation-17. They compared the data for three size ranges for $0.2 - 0.7\mu m$, $0.7 - 7\mu m$, and $7 - 90\mu m$ by regression analyses. The results of their analyses suggested a value of about *N=84*, (for $\delta_1 + \delta_2 = 0.1158\mu m$).

Based on the measured values of surface roughness for graphite (0.121 μm), we selected a suitable value for *N*, by using extrapolation technique for the data from the work of Wolff and Schneider. Taking the value of other parameters in equation-7 for air, the joint thermal resistance was calculated for graphite samples using equation-14. Finally the total thermal resistance for this material was calculated using equations 4 and 5.

Computations results and discussions

The total thermal resistance estimated for the aluminum sample using equation-16 for different cases is shown in table-3 below. For all the cases studied using the theoretical model the thermal resistance model slightly overestimates the values.

Table 3 Theoretically estimated values of total thermal resistances for aluminum samples.

Sample type	Thermal resistance (K/W)	Error (%)
Aluminum pieces in direct contact	3.751	4.9
Aluminum pieces with graphite interface	0.889	5.6
Aluminum pieces with CNT interface	0.778	5.8

For the case of aluminum pieces in direct contact as the micro-contact resistance (R_c) is much greater than the micro-gap resistance (R_g), the joint resistance R_j is primarily dependent on R_g . Since the micro-gap is filled with air with a low thermal conductivity value a high value of thermal contact resistance is obtained in this case. For the case with graphite coating, it was assumed some of the graphite particles fill the micro-gaps, which lowered down R_c and also due the presence of graphite particles in the micro-gap the conductivity value k_g was taken as the harmonic mean of the air and graphite particle conductivity. This further lowered down R_g which resulted in the reduction in the joint resistance R_j . For the case of aluminum pieces with CNT TIM the micro-contact at the aluminum and TIM material produced a low thermal resistance due to the high thermal conductivity of the CNT sheet. Also it was assumed that the retention of CNT in the micro-gaps affects the value k_g , which reduced the value of R_g and eventually the value of R_j . The total thermal resistance values obtained for all cases using the theoretical model were within 6 % error as compared with experimental values.

The total thermal resistances values for graphite samples for different cases are shown in table 4 below. The values for gap coefficients *N* to calculate the effective distance between surfaces δ were estimated by extrapolating the data from regression analysis of [39]. Accordingly the values of *N* were taken as 92 for graphite.

Table 4 Theoretically estimated values of total thermal resistances for graphite samples.

Sample type	Thermal resistance (K/W)	Error (%)
Graphite pieces in direct contact	2.658	5.4
Graphite pieces with graphite interface	0.720	6.0
Graphite pieces with CNT interface	0.598	6.4

For graphite samples the model for polished surfaces predicted an overestimation in total thermal resistance values. The thermal contact resistance from equation-25 depends on the conductance number *U*, the fluid thermal conductivity k_f , and the effective distance between surfaces δ . The importance of having good conforming surfaces is clearly emphasized by the fact that this can lead to the minimizing of δ . Also with such surfaces a high thermal conductivity TIM can become more effective by providing a greater heat transfer path.

Conclusions

An experimental analysis was conducted using a modern laser flash device to measure the effective thermal conductivity of aluminum and graphite for different cases: in direct contact, with a graphite coating and with a CNT TIM. The inclusion of graphite coating and thin sheet of CNT TIM showed considerable reduction in thermal resistance values for both materials. In order to compare the experimental results with the theoretical models from literature two thermal resistance models were selected. The values of total thermal resistances using both models showed reasonable agreement with the experimental results with an error of less than 6.5 %. From the experimental and theoretical studies it was established that two factors

namely the presence of conforming surfaces and high thermal conductivity path are extremely important for lowering the thermal contact resistance. For both aluminum and graphite the presence of micro-gaps was the main factor in the high thermal contact resistance. The graphite spray coating filled the gaps to certain extent and also created a greater conductivity at the micro-contact thereby lowering down the thermal resistance. However, the CNT TIM proved to be more effective by further lowering down the thermal contact resistance and improving the thermal contact conductance for both the materials analyzed. An important factor which can further improve the performance of the CNT TIM is its wettability. The use of phase change materials with high wetting characteristic can be used along with the CNT to form an even better conforming contact. This can further lower down the thermal interface resistance value by reducing or even eliminating the micro air gaps at the interface.

References

Berber S, Kwon Y. K, Tomanek D. 2000. Unusually high thermal conductivity of carbon nanotubes, *Physics Review Letters* 84(20): 4613–4617.

Che J. W, Cagin T, Goddard W. A. 2000. Thermal conductivity of carbon nanotubes, *Nanotechnology* 11(2): 65–69.

Choi S. U. S, Zhang Z. G, Yu W, Lockwood F. E, Grulke E. A. 2001. Anomalous thermal conductivity enhancement in nanotube suspensions, *Applied Physics Letters* 79(14): 2252–2254.

Grujicic M, Zhao C. L, Dusel E. C. 2005. The effect of thermal contact resistance on heat management in the electronic packaging. *Applied Surface Science* 2005 246:290–302.

Huxtable ST, Cahill DG, Shenogin S, Xue L, Ozisik R, Barone P, Usrey M, Strano MS, G. Siddons, Shim M, Keblinski P. 2003. Interfacial heat flux in carbon nanotube suspensions, *Nature Materials* 731–734.

Kim P, Shi L, Majumdar A, McEuen P. L. 2001. Thermal transport measurements of individual multiwalled nanotubes, *Physics Review Letters* 87: 215502-1–215502-4.

Luo X, Chugh R, Biller B. C, Hoi Y. M, Chung D. D. L. 2002. Electronic applications of flexible graphite. *Journal of Electronic Materials* 31(5):535–44.

Maruyama S. 2003. A molecular dynamics simulation of heat conduction of a finite length single-walled carbon nanotube, *Microscale Thermophysics Engineering* 7: 41–50.

Ochterbeck J. M, Peterson G. P, Fletcher L. S. 1991. Thermal contact conductance of metallic coated BiCaSrCuO super conductor:copper interfaces at cryogenic temperatures. *ASME/JSME Thermal Engineering Proceedings* 1: 275-84.

Ouellette T, de Sorgo M. 1985. Thermal performance of heat transfer interface materials. *In: Proceedings of the power electronics design conference, power sources users conference, Cerritos, CA* 34–38.

Peterson A. L. 1990. Silicones with improved thermal conductivity for thermal management in electronic packaging. *Proceedings of the 40th electronic components and technology conference, Piscataway, NJ: IEEE* 1: 613–619.

Sartre V, Lallemand M. 2001. Enhancement of thermal contact conductance for electronic systems. *Applied Thermal Engineering* 21:221–235.

Sasaski T, Hisano K, Sakamoto T, Monma S, Fijmori Y, Iwasaki H, et al. 1995. Development of sheet type thermal conductive compound using AlN. *In: Symposium proceedings, IEEE/CPMT international electronic manufacturing technology (IEMT) symposium. Piscataway, NJ: IEEE* 236–239.

Savija, I., Culham, J. R., Yovanovich, M. M., and Marotta, E. E. 2002. Review of Thermal Conductance Models for Joints Incorporating Enhancement Materials, *40th AIAA Aerospace Sciences Meeting and Exhibit (AIAA-2002-0494), Reno, NV.*

Teertstra, P., Yovanovich, M. M., Culham, J. R., and Lemczyk, T. 1999. Analytical Forced Convection Modelling of Plate Fin Heat Sinks, *Proceedings of the Fifteenth Annual IEEE Symposium on Semiconductor Thermal Measurement and Management, San Diego, CA* 34-41.

Veziroglu T. N. 1967. Correlation of thermal contact conductance experimental results. *Progress in Astronautics and Aeronautics. Academic Press, New York.*

Vogel M. R. 1995. Thermal performance for a miniature heat sink cooled by microPCM slurry. *Proceedings of the international intersociety of electronic packaging conference, advances in electronic packaging. American Society of Mechanical Engineers* 10: 989.

Wilson S. W, Norris A. W, Scott E. B, Costello M. R. 1996. Thermally conductive adhesives for high thermally stressed assembly. *National electronic packaging and production conference, proceedings of the technical program, Norwalk, CT* 2: 788–96.

Wolff E. G, Schneider D. A. 1998 Prediction of thermal contact resistance between polished surfaces. *International Journal of Heat and Mass Transfer* 41(22): 3469–82.

Xu Y, Luo X, Chung D. D. L. 2000. Sodium silicate based thermal pastes for high thermal contact conductance. *Journal of Electronic Packaging* 122(2): 128–131.

Xu Y, Luo X, Chung D. D. L. 2002. Lithium doped polyethylene-glycolbased thermal interface pastes for high thermal contact conductance. *Journal of Electronic Packaging* 124(3):188–191.

Xu J, Fisher T. S. 2004. Enhanced thermal contact conductance using carbon nanotube arrays, in: ITherm 2004 Proceedings: Ninth Intersociety Conference on Thermal and Thermomechanical Phenomena in Electronic Systems, Las Vegas, NV 549– 555.